IEEE Access
Multidisciplinary | Rapid Review | Open Access Journal

Received February 21, 2019, accepted March 8, 2019, date of publication March 21, 2019, date of current version May 3, 2019.

Digital Object Identifier 10.1109/ACCESS.2019.2906866

NLOS Identification and Correction Based on Multidimensional Scaling and Quasi-Accurate Detection

YUHONG ZHU[1], TENGFEI MA[1], ZHIJUN LI[1], DAYANG SUN[1], XIAOSONG SUN[2], XIAOHUI ZHAO[1], AND FENGYE HU[1]

[1]College of Communication Engineering, Jilin University, Changchun 130012, China
[2]Mathematics School and Institute, Jilin University, Changchun 130012, China

Corresponding author: Fengye Hu (hufy@jlu.edu.cn)

This work was supported in part by the Jilin Provincial Science and Technology Department Key Scientific and Technological Project under Grant 20190302031GX, in part by the Changchun Scientific and Technological Innovation Double Ten Project under Grant 18SS010, in part by the National Natural Science Foundation of China under Grant 61671219, and in part by the Jilin Province Development and Reform Commission Project under Grant 2017C046-3.

ABSTRACT In wireless sensor networks, most of the previous NLOS identification is based on error estimation model established by raw data. In this paper, we propose a method of NLOS identification named NIMQ based on multidimensional scaling (MDS) and Quasi-Accurate detection (QUAD). In this method, we first map NLOS information into gross error information by MDS, then we use QUAD to identify the gross errors which contain the NLOS information. This method relies only on distance measurements and is independent of the measured error estimation model. In addition, using the network topology constraints in higher dimensional space, the identified distance can be corrected by multiple iterations. Finally, an NLOS iterating correction algorithm (NICA) is proposed. Simulations show that in different scenarios our proposed NIMQ and NICA can well identify and correct NLOS measurement.

INDEX TERMS NLOS identification, NLOS correction, MDS, gross error.

I. INTRODUCTION

In indoor positioning, the placement constantly changes [23]. Due to the obstruction of middle obstacle, the radio waves are distorted by the diffraction between a pair of nodes, which makes the measured distance between these two nodes larger than its true value [4], [16]. This is a non-line-of-sight (NLOS) problem and is ubiquitous [15].

In the study of wireless sensor network (WSN) and 5G small cells, the research on the NLOS problem mainly includes the state identification of NLOS and the error mitigation of NLOS [7], [13], [26], [28], [29].

At present, the NLOS identification mainly uses the error estimation model [7], [15], [27]–[29], the dependent parameters are time of arrive (TOA) [1], [5], [10], [25], [26], phase difference of arrival (PDOA) [12], [24], received signal strength (RSS) [9], [18], [20], or channel state information (CSI) [3], [8], [19]. However, the identification of NLOS based on these measured data has a large time overhead, usually in an exponential relation with the number of stations [15]. In fact, we can use only measured distances to identify NLOS measurements in large scale networks. Instead of the error mitigation, we can also do correction of NLOS measurements based on the constraint relation in geometric topology.

Additionally, a large number of sensors deployed in positioning system deployment generates lots of raw data, which will inevitably produce gross measurement error [11]. It will make the measurements far from true values. To identify and eliminate the gross errors or correct them, the only information we can use is the measured data. Fortunately, many contributions in the gross error identification can be found in the past decades. For example, the theory of residues [6], [14], [17] can be employed here to gain useful results.

Intuitively, the problem of NLOS identification is similar to the problem of the gross error identification so that we can use theories and results of gross error to solve the problem of NLOS. However, there is difference between NLOS identification and gross error identification in details. We know

The associate editor coordinating the review of this manuscript and approving it for publication was Gongbo Zhou.

that gross error is the deviation under the same measurement conditions, while for NLOS identification, the conditions are different with each distance measurement. If we establish a model to map the NLOS problem into the gross error problem, the results achieved in the gross error problem can be utilized to do NLOS identification.

The method of multidimentional scaling (MDS) can be used in the mapping problem. MDS [2], [21], [22] is a kind of transformation method to produce relative coordinates from a squared distance matrix in any dimensional space. Based on this method, we can treat the coordinates in high dimensional space as raw data under the same measurement conditions. Thus we can map the problem of NLOS identification into the problem of gross error identification.

The contributions of this paper are as follows.

- Based on the MDS theory, we propose a method which does not rely on the measured error estimation model, but only uses the geometric topology constraints of nodes to identify NLOS distance in large-scale networks.
- For the gross error identification, we use Quasi-Accurate Detection [17] which is a gross error identification method based on true errors and definite analytic relationship between the true error and the observed value. The method is accurate and reliable according to the distribution characteristic of true error estimation. It can effectively locate multiple gross errors and closely assess the evaluation accuracy [17].
- We propose an NLOS correction method to make more efficient use of geometric topology constraints in large scale networks. Using this method, the NLOS value can be gradually corrected to the true value by iterating it several times until a precision threshold is reached.

The rest of this paper is organized as follows: the mathematical model is established in Section 2, and based on this model, Section 3 proposes the NLOS identification algorithm NIMQ. After that, Section 4 proposes an algorithm named NLOS iterating correction algorithm NICA, and Section 5 concludes the paper.

II. MATHEMATICAL MODEL OF NLOS IDENTIFICATION

We suppose there are N isomorphic nodes in an indoor positioning system. When we use ToA, TDoA or ultrasound technologies, the measured distance $\tilde{d}_{ij}$ between node i and node j can be derived. Thus these N^2 measured distances of N nodes constitute a N-dimensional raw data matrix

$$\tilde{D} = \begin{pmatrix} \tilde{d}_{11} & \tilde{d}_{12} & \cdots & \tilde{d}_{1N} \\ \tilde{d}_{21} & \tilde{d}_{22} & \cdots & \tilde{d}_{2N} \\ \vdots & \vdots & \ddots & \vdots \\ \tilde{d}_{N1} & \tilde{d}_{N2} & \cdots & \tilde{d}_{NN} \end{pmatrix} \tag{1}$$

Let $\tilde{D}$ be composed of true values and measured errors as

$$\tilde{D} = D + \Delta D \tag{2}$$

where

$$D = \begin{pmatrix} d_{11} & d_{12} & \cdots & d_{1N} \\ d_{21} & d_{22} & \cdots & d_{2N} \\ \vdots & \vdots & \ddots & \vdots \\ d_{N1} & d_{N2} & \cdots & d_{NN} \end{pmatrix} \tag{3}$$

is the martix of true distances, and

$$\Delta D = \begin{pmatrix} \Delta d_{11} & \Delta d_{12} & \cdots & \Delta d_{1N} \\ \Delta d_{21} & \Delta d_{22} & \cdots & \Delta d_{2N} \\ \vdots & \vdots & \ddots & \vdots \\ \Delta d_{N1} & \Delta d_{N2} & \cdots & \Delta d_{NN} \end{pmatrix} \tag{4}$$

is the matrix of measured errors.

Since all nodes in this indoor positioning system are isomorphic, we suppose that the true distance d_{ij} equals to d_{ji}, hence D is symmetric.

In this indoor positioning environment, if there is an obstacle between two nodes, we have NLOS distance measurements in $\tilde{D}$. To simplify NLOS identification problem, we assume that only one pair of distances is NLOS distance measurement, namely $\tilde{d}_{ij}$ and $\tilde{d}_{ji}$. Now our problem becomes identifying which distance measurement is the NLOS one by the given $\tilde{D}$ and correcting the NLOS measurement to its true value.

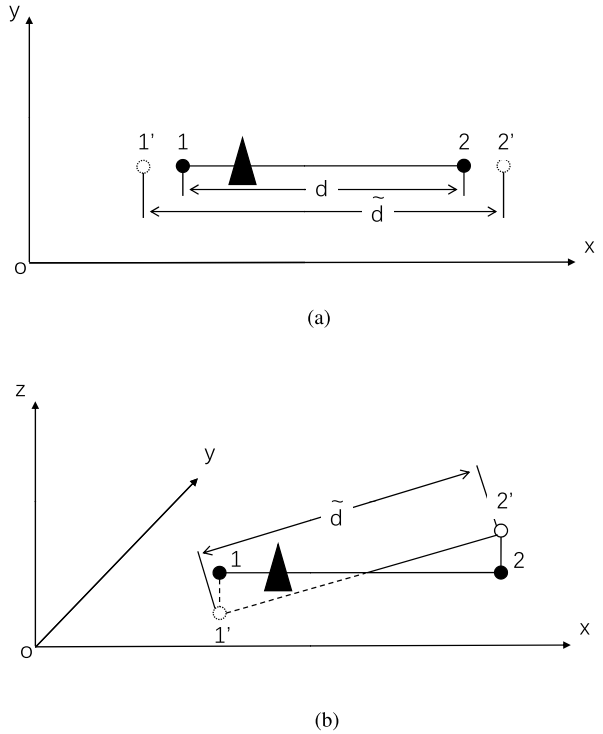

FIGURE 1. Dimension extension. (a) 2-dimension. (b) 3-dimension.

In order to clearly explain the idea of this paper, we give an intuitive illustration in Fig.1. We suppose there are only two nodes in a positioning scenario and an obstacle between them. The true distance between these two nodes is d and the measured one is $\tilde{d}$. If we solve this problem in 2-dimensional

space using optimization method such as the least square (LS) algorithm, we can get the coordinates as shown in Fig.1(a). However, if this problem is solved in 3-dimensional space as shown in Fig.1(b), the coordinates of the projection in the original 2-dimensional space could be more accurate than those in Fig.1(a). The longer the distance is measured, the bigger the 3rd coordinate is. Therefore, this mapping from the measured distances to the coordinates can be used to identify which measured distance is the most inaccurate one.

In a 2-dimensional space, for $\tilde{D}$ with N nodes, to find the coordinates, the 2-dimensional planar coordinates can be extended to 3-dimensional space by a matrix X, under the assumption that the third extended dimension is a matrix Z as follows.

$$X = \begin{pmatrix} X_1 \\ X_2 \\ \vdots \\ X_N \end{pmatrix} = \begin{pmatrix} x_1 & y_1 & z_1 \\ x_2 & y_2 & z_2 \\ \vdots & \vdots & \vdots \\ x_N & y_N & z_N \end{pmatrix} \tag{5}$$

$$Z = \begin{pmatrix} z_1 \\ z_2 \\ \vdots \\ z_N \end{pmatrix} \tag{6}$$

When the distances in $\tilde{D}$ are all true ones, there are no measured errors, which means that the elements of X in Z-field noted as Z should be all zeroes. If we introduce a small measured error to one of the distances, the elements of Matrix X in Z-field vary. The Z-field coordinates reflect the total size of general error and the gross deviation. In this way, the measured error in $\tilde{D}$ is converted to the Z-field of X. Then we can estimate the gross error in Z-domain for the identification of the NLOS distance in $\tilde{D}$.

To make further verification, we conduct some experiments to see whether Z-field reflects the gross error. For a planar topology shown in Fig.2, the true distance between node 5 and node 11 is 83. We use MDS to calculate the coordinates. When we introduce a gross error making the distance to 100, Fig.3 shows an intuitive result that there are 2 peaks at node 5 and node 11 in Z-field. When we introduce another gross error making the distance to 60, less than its true value in the experiment, we find that node 5 and node 11 can still reflect the gross error in Fig.4. Interestingly, when the measured distance introduced is longer than its true value the 2 peaks noted by node 5 and node 11 are on different sides of in Fig.3, and when the measured distance introduced is shorter than its true value the 2 peaks noted by node 5 and node 11 are on the same side of Fig.4.

III. NLOS IDENTIFICATION BASED ON MDS AND QUAD

A. MDS PROCESS

For indoor positioning, MDS can be used to obtain coordinates in higher-dimensional space, so that higher dimension can be treated as raw data with gross error. A square distance

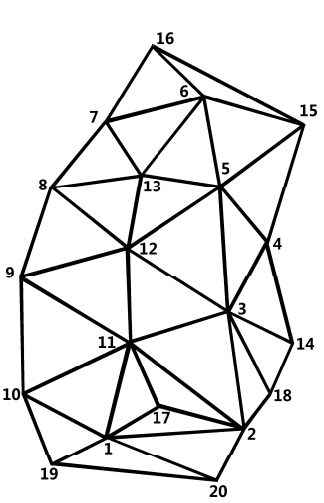

FIGURE 2. Planar layout.

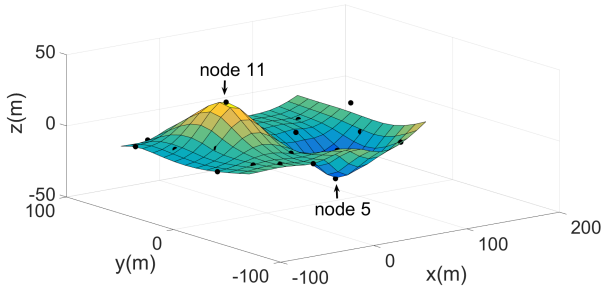

FIGURE 3. Three-dimensional topology with gross error greater than true value.

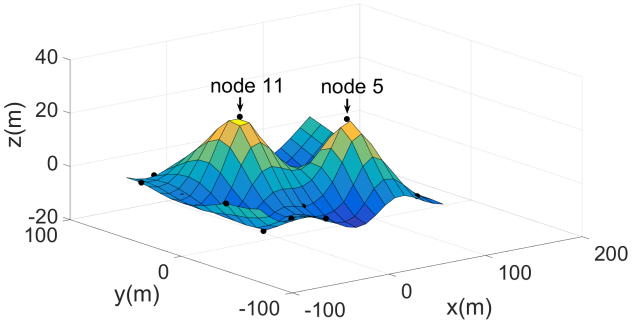

FIGURE 4. Three-dimensional topology with gross error less than true value.

matrix is used in MDS as follows [2], [21], [22]

$$\tilde{D}^{(2)} = \begin{pmatrix} \tilde{d}_{11}^2 & \tilde{d}_{12}^2 & \cdots & \tilde{d}_{1N}^2 \\ \tilde{d}_{21}^2 & \tilde{d}_{22}^2 & \cdots & \tilde{d}_{2N}^2 \\ \vdots & \vdots & \ddots & \vdots \\ \tilde{d}_{N1}^2 & \tilde{d}_{N2}^2 & \cdots & \tilde{d}_{NN}^2 \end{pmatrix} \tag{7}$$

Multiplying the left and the right sides of $\tilde{D}^{(2)}$ by a centering matrix $P = I - 11'/N$ and a factor -1/2 gives

$$-1/2P\tilde{D}^{(2)}P = B \tag{8}$$

where I is the unit matrix, $11'$ is the all 1 matrix. Then, to find the MDS coordinates from B, we factor B through the eigen-decomposition

$$B = Q\Lambda Q' = (Q\Lambda^{1/2})(Q\Lambda^{1/2})' \tag{9}$$

where Q is the eigenvector matrix and Λ is the eigenvalue matrix.

Let the matrix of the first m eigenvalues greater than zero be Λ_+, and Q_+ be the first m columns of Q, then the relative coordinates of the nodes can be written as

$$X = Q_+\Lambda_+^{1/2} \tag{10}$$

where X has a total of N rows and m columns. Each row of X represents the relative coordinate value of a node in m-dimensional space.

In [21], we know that MDS can be used to estimate the coordinates in 2-dimensional space. In fact, if $D^{(2)}$ is the true distances which can be derived from coordinates X in 2-dimensional space, we have

$$rank(-1/2PD^{(2)}P) = rank(B) \tag{11}$$

Since $rank(B) = rank(XX') = rank(X) = 2$, there are only 2 positive eigenvalues in eigen-decomposition of B, so that the coordinates we get are in 2-dimensional space.

However, when we introduce NLOS measurement to $D^{(2)}$, the rank of $1/2P\tilde{D}^{(2)}P$ could increase. In our experiments, eigenvalues of $1/2P\tilde{D}^{(2)}P$ could be 4 or more, therefore we can get the coordinates in higher dimensions. Base on this result, we will explore the coordinate estimation in 3-dimensional space.

B. PRINCIPLE OF NLOS IDENTIFICATION

In the proposed mathematical model, we suppose that matrix $\tilde{X}$ is the coordinates derived from $\tilde{D}$ by MDS, and X is the coordinates derived from D, let

$$\tilde{X} = X + \Delta X \tag{12}$$

For any real matrix A, we know that its Euclid norm is $\|A\|_2 = \sqrt{\Lambda_1}$, where Λ_1 is the maximum eigenvalue of $A'A$. Then we have following useful result.

For any $m \times n$ real matrix A, $\|A'\|_2 = \|A\|_2$, since $|\lambda I_n - A'A| = \lambda^{n-m}|\lambda I_n - AA'|$, which means $A'A$ and AA' have same non-zero eigenvalues.

In addition, for any real symmetric matrix A, $\|A'A\|_2 = \|A\|_2^2 = \|A'\|_2^2$, since for a real symmetric matrix A, the eigenvalues of $A^2 = A'A$ is the square of the eigenvalues of A.

Based on the above results, the principle of NLOS identification can be concluded in the following two lemmas.

Lemma 1: For $\tilde{X} = X + \Delta X$ derived from $\tilde{D} = D + \Delta D$ and X derived from D using MDS,

$$|\|X + \Delta X\|_2 - \|X\|_2| \le \frac{1}{\sqrt{2}}\|\Delta D^{(2)}\|_2^{\frac{1}{2}} \tag{13}$$

The proof of this lemma is in Appendix A.

Lemma 2: For $\tilde{X} = X + \Delta X$ derived from $\tilde{D} = D + \Delta D$ and X derived from D using MDS, if there is only one distance error in ΔD which can be written as

$$\Delta D^2 = \begin{pmatrix} 0 & 0 & \cdots & 0 \\ 0 & \ddots & \Delta d_{ij}^2 & 0 \\ \vdots & \Delta d_{ij}^2 & \ddots & \vdots \\ 0 & 0 & \cdots & 0 \end{pmatrix} \tag{14}$$

then,

$$|\|X_t + \Delta X_t\|_2 - \|X_t\|_2| \le \begin{cases} \sqrt{1/2\|\frac{1}{N^2}\Delta\tilde{d}_{ij}^2 + \frac{1}{N^2}\Delta\tilde{d}_{ji}^2\|}, & t \ne i, t \ne j. \\ \sqrt{1/2\|(1-\frac{1}{N})^2\Delta\tilde{d}_{ij}^2 + \frac{1}{N^2}\Delta\tilde{d}_{ji}^2\|}, & t = i. \\ \sqrt{1/2\|\frac{1}{N^2}\Delta\tilde{d}_{ij}^2 + (1-\frac{1}{N})^2\Delta\tilde{d}_{ji}^2\|}, & t = j. \end{cases} \tag{15}$$

The proof of this lemma is in Appendix B.

From Lemma 2, we can see that there is an inequality relationship among ΔX_i, ΔX_j and $\Delta\tilde{d}_{ij}$, $\Delta\tilde{d}_{ji}$. It implies that when N is big enough, the NLOS measurement $\tilde{d}_{ij}$ and $\tilde{d}_{ji}$ will be reflected in the coordinates of node i and node j. That is why we can use QUAD to identify the NLOS measurements in higher dimension.

C. PRINCIPLE OF GROSS ERROR IDENTIFICATION

For indoor positioning problems with NLOS measurements, if an NLOS measurement is treated as a true value, there is an exact solution in high-dimensional space and the NLOS deviation will be reflected in the data of this space. Therefore, we can identify the NLOS measurement if we can identify the deviation in high-dimensional space. We define the following linear equation

$$AX_0 = L + \Delta \tag{16}$$

whose evaluation form is

$$AX^t = L + V \tag{17}$$

where A is the $N \times M$ coefficient matrix whose rank is m and dimension is $n \times m$. X_0 is the m-dimensional vector to represent the true value of the position parameter, X^t is the estimate of X_0, L is the n-dimensional observation vector, Δ is the error of the observed vector, and V is the residual of the observed value L [17].

A definite relationship between Δ and L is

$$A\Delta = -RL \tag{18}$$

which can be treated as a linear system for Δ, where $R = I - J$ is the orthogonal projection of J, and $J = A(A^TA)^{-1}A^T$ is the adjustment factor matrix.

If we consider a topology with n nodes in 2-dimensional space, we can calculate the coordinates in 3-dimensional

space (we treat the 3rd dimension as Z dimension). Using this QUAD process on the calculated coordinates, we have

(1)The true values of Z are all 0;

(2)Every weight of Z is the same, we can set A with all 1;

(3)Z is used as the measurement value of L and is introduced to the QUAD algorithm for calculation.

Since the number of identified gross errors may be two, three or more, we first consider the simplest case with only two gross errors.

D. NLOS IDENTIFICATION ALGORITHM BASED ON MDS AND QUAD(NIMQ)

We suppose there are N nodes and only one NLOS measurement in a plane indoor positioning scenario. To identify the NLOS measurement, our algorithm needs to check the validity of the input distance matrix first to ensure that the input distance matrix is available. Then, MDS algorithm is performed on the squared distance matrix in 3-dimensional space and the third dimension Z-field is derived. Then, the coordinates in 3-dimensional space are introduced in QUAD algorithm to obtain the nodes' index of the NLOS measurement. It is noteworthy that, in the initialization of QUAD, A is initialized to all 1 matrix. The process of NLOS identification algorithm is shown in Fig.5.

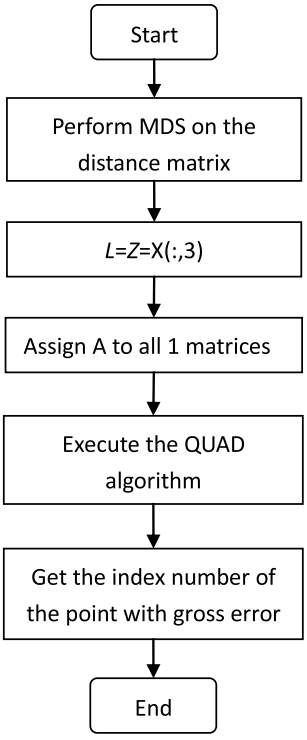

FIGURE 5. Identification process.

To verify this NLOS identification algorithm, we conduct the experiments under random topology, grid topology, L-type topology, and C-type topology as shown in Fig.6.

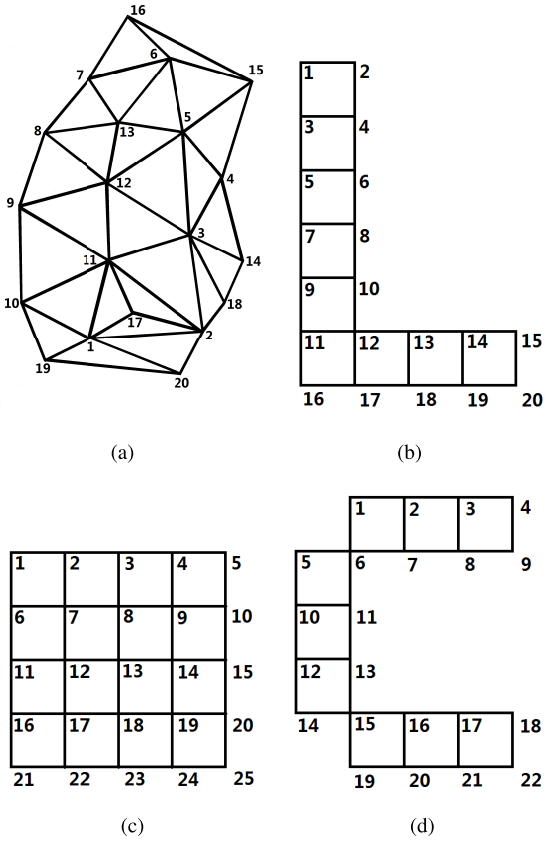

FIGURE 6. Planar Topologies. (a) random. (b) L-type. (c) grid. (d) C-type.

The original data used in our experiments are actually measured manually, and the error of the manual measurement simulates the natural error of the radio wave measurement between two nodes. For the topology in Fig.6(a), we randomly select 20 nodes in a plane, and the distances between the nodes are measured with millimeter unit in order to form an original distance matrix (19).

$$\tilde{D} = \begin{pmatrix} 0 & 65 & 82 & 118 & 129 & \cdots & 56 \\ 65 & 0 & 55 & 88 & 114 & \cdots & 28 \\ 82 & 55 & \cdots & \cdots & \cdots & \cdots & \vdots \\ 118 & 88 & \cdots & \cdots & \cdots & \cdots & \vdots \\ 129 & 114 & \cdots & \cdots & \cdots & \cdots & \vdots \\ \vdots & \vdots & \vdots & \vdots & \vdots & \ddots & \vdots \\ 56 & 28 & \cdots & \cdots & \cdots & \cdots & 0 \end{pmatrix} \tag{19}$$

Moreover, in the experiments, we introduce NLOS measurement into the distance between node 1 and node 20 in $\tilde{D}$ as the gross error. The distance increases from 56 to 120 to conduct a simulated distance matrix $\tilde{D_m}$ as shown in

TABLE 1. Coordinates by MDS.

X	Y	Z	4th dimension	5th dimension
-67.4348	28.0865	(50.6986)	0.4331	-0.3157
-63.5032	-41.533	4.9456	-10.9352	10.8237
-9.695	-30.6894	4.0555	0.8534	-1.4541
23.9423	-44.68	4.1368	-0.8592	-3.8347
47.7895	-21.4708	-0.8953	-0.0158	-7.8897
89.1502	-10.1945	1.3389	-6.63	-3.6413
73.3454	33.7756	-4.9357	-3.6982	-1.4269
40.1529	56.5019	-7.9121	-2.976	0.6601
-1.5205	67.4989	-7.587	-2.1049	4.3603
-57.0801	62.0142	-5.1806	-4.737	-7.9786
-26.7703	13.2973	-1.6832	13.5729	6.2888
15.3358	18.8912	-2.7026	3.2568	-1.7434
48.6631	15.1409	-0.1394	-12.1979	6.852
-20.9929	-60.8317	7.0558	0.5345	0.2455
78.8449	-56.4343	5.1406	3.7313	-4.6105
109.2925	16.056	-2.5557	12.4573	7.9618
-57.4107	-2.0471	1.6417	5.3378	0.7525
-47.3856	-52.6325	5.8624	-0.0386	0.5971
-89.7752	45.258	-2.0484	3.9584	-5.5448
-84.9483	-36.0071	(-49.236)	0.0574	-0.1021

Matrix (20).

$$\tilde{D}_m = \begin{pmatrix} 0 & 65 & 82 & 118 & 129 & \cdots & (120) \\ 65 & 0 & 55 & 88 & 114 & \cdots & 28 \\ 82 & 55 & \cdots & \cdots & \cdots & \cdots & \vdots \\ 118 & 88 & \cdots & \cdots & \cdots & \cdots & \vdots \\ 129 & 114 & \cdots & \cdots & \cdots & \cdots & \vdots \\ \vdots & \vdots & \vdots & \vdots & \vdots & \ddots & \vdots \\ (120) & 28 & \cdots & \cdots & \cdots & \cdots & 0 \end{pmatrix} \tag{20}$$

We transform $\tilde{D}_m$ by MDS, and obtain the coordinates given in Table 1. The intuitive topology from Table 1 as X in 3-dimensional space is shown in Fig.7(a).

The QUAD gross error identification is performed on each column respectively, and the gross error index number matrices are recorded as R_x, R_y, R_z as shown in Table 1 in brackets.

In order to choose the dimension of data information of the coarse error, we examine the size of R_x, R_y and R_z in order. If one of them has a size of 2 and the corresponding values of the two indices are obviously beyond the mean value in the field, the gross error data information can be locked with this dimension. Therefore, the position of the gross error is determined. We give several experiment results by introducing different NLOS measurements into the topologies. In the experiments, a dozen distances are introduced in the NLOS measurements. After MDS and QUAD, the results presented in Table 2 show that it is efficient to identify these NLOS measurements by NIMQ.

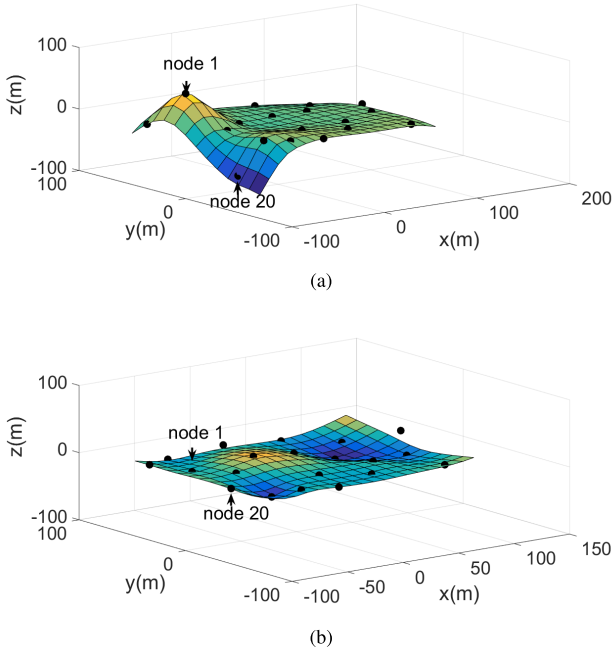

FIGURE 7. Comparison of random topology. (a) original random topology. (b) random topology by NICA.

IV. NLOS CORRECTION

A. NLOS ITERATING CORRECTION ALGORITHM (NICA)

In a deterministic network topology, nodes are mutually constrained with each other. By using the mutual relations between these nodes, it is possible to correct the distance with gross errors under the supervision of constraint relationship.

TABLE 2. Identification of gross errors.

(Point1,Point2)	true value	value after gross error is introduced	identified results
(1,20)	56	120	1,20
(3,8)	101	160	3,8
(11,13)	78	140	11,13
(2,12)	100	150	2,12
(5,9)	102	170	5,9
(9,11)	60	100	9,11
(5,6)	43	80	5,6
(3,12)	55	100	3,12
(14,17)	70	180	14,17
(2,4)	88	200	2,4
(6,15)	48	200	6,15
(1,9)	85	240	1,9

TABLE 3. NLOS iterating correction algorithm (NICA).

Algorithm 1 NICA

Input: $\tilde{D}$, nodes' index m, n and threshold t
Output: corrected distance d_{mn}
Step 1 Set initial value of d_l to 0, and initial value d_h to $\tilde{d}_{mn}$.
loop
  Step 2 $\tilde{d}_{mn} = (d_l + d_h)/2$
  Step 3 perform MDS transformation with modified $\tilde{D}$ to get z_m and z_n.
  Step 4
    if z_m and z_n have opposite sign,
      $d_h = d_{mn}$
    else
      $d_l = d_{mn}$
    endif

    if $d_h - d_l < t$,
      return $\tilde{d}_{mn}$
    endif
end loop

From the experiments in Section 2, we know that the measured error can be reflected in higher dimensions. The experiment results given in Fig.3 and Fig.4 shows that when the measurement is bigger than the true distance, the 2 peaks are on different sides of the original plane, and when the measurement is smaller than the true distance, the 2 peaks are on the same side of the original plane. This important property can be used to correct the NLOS measurement to its true distance.

We assume that the distance to be corrected is $\tilde{d}_{mn}$, the true distance is d_{mn} and the Z-coordinate of the two points in X is z_m,z_n respectively. If $\tilde{d}_{mn}$ is an NLOS measurement, it should be bigger than d_{mn} where d_{mn} satisfies

$$d_{mn} \in (0, \tilde{d}_{mn})$$

According to our experiments, if z_m and z_n have opposite signs, indicating $\tilde{d}_{mn} > d_{mn}$, we should reduce d_{mn}. If z_m and z_n have the same sign, indicating $\tilde{d}_{mn} < d_{mn}$, we should increase d_{mn}. Hence, we propose an iterative algorithm to correct the NLOS distance in Table 3, and the process of the algorithm is shown in Fig.8. The final result of the correction will make $\tilde{d}_{mn}$ approximate d_{mn}.

B. EXPERIMENTS RESULTS AND ANALYSIS

Our experiments are carried out with 4 typical topologies, random topology, L-type topology, grid topology, and C-type topology shown in Fig.6 to verify the validity of NICA for different topological networks. Fig.7, Fig.10, Fig.9, and Fig.11 show the comparisons before and after NICA is applied in 3-dimensional space with these topologies respectively. In these results, Fig.7(a), Fig.10(a), Fig.9(a), and Fig.11(a) are original three-dimensional coordinate graphs. Within the same coordinate scale, we can see from these figures that there exist obvious distance gross errors in Z-domain. After NICA is applied, we can see from Fig.7(b), Fig.10(b), Fig.9(b), and Fig.11(b), that the distance gross errors are corrected and the topologies are restored into 2-dimension topologies.

The process of NICA shows more details about these corrections. Take random topology shown in Fig.7 for example, after we conduct MDS on this topology, we get the coordinates shown in Table 1. From the results in this table, we find that the NLOS information is transformed from the distance

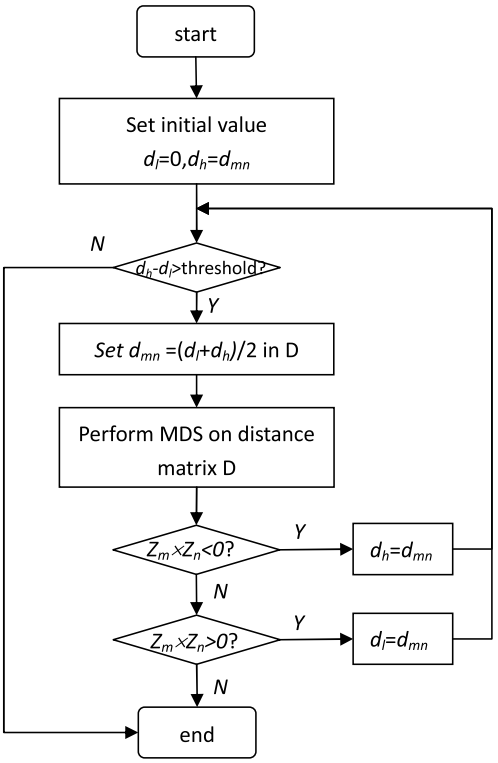

FIGURE 8. Process of NLOS iterating correction algorithm.

$$\tilde{D}'_m = \begin{pmatrix} 0.0 & 65.0 & 82.0 & 118.0 & 129.0 & \cdots & (56.54) \\ 65.0 & 0.0 & 55.0 & 88.0 & 114.0 & \cdots & 28.0 \\ 82.0 & 55.0 & \cdots & \cdots & \cdots & \cdots & \vdots \\ 118.0 & 88.0 & \cdots & \cdots & \cdots & \cdots & \vdots \\ 129.0 & 114.0 & \cdots & \cdots & \cdots & \cdots & \vdots \\ \vdots & \vdots & \vdots & \vdots & \vdots & \ddots & \vdots \\ (56.54) & 28.0 & \cdots & \cdots & \cdots & \cdots & 0.0 \end{pmatrix} \quad (21)$$

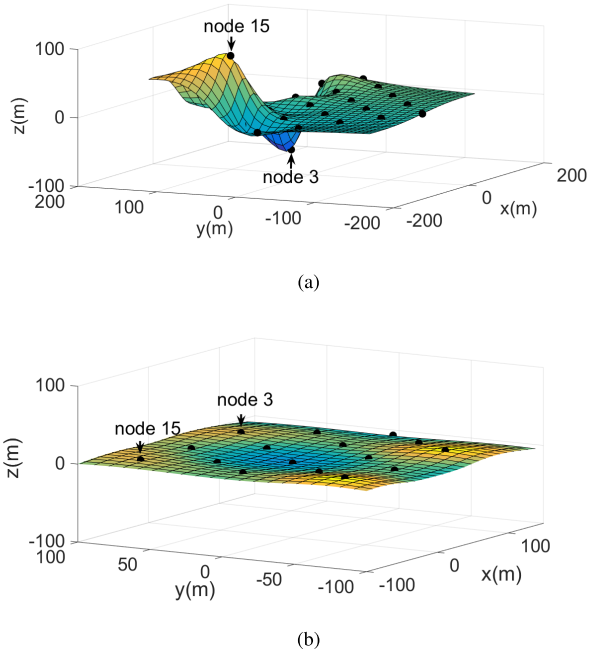

FIGURE 9. Comparison of grid topologies before and after correction. (a) before correction. (b) after correction.

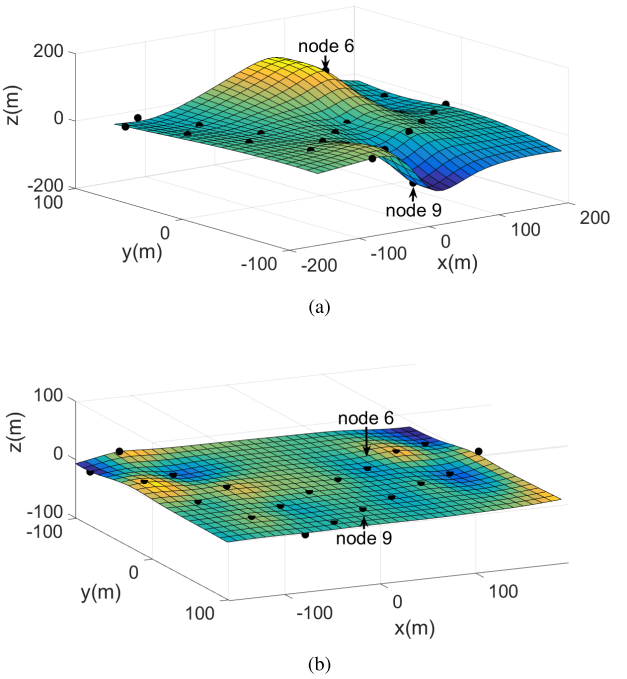

FIGURE 10. Comparison of L-type topologies before and and after correction. (a) before correction. (b) after correction.

matrix D to Z, and there is an NLOS distance obviously. We also find that the distance between node 1 and node 20 is NLOS. Using QUAD, we can accurately locate the position where the gross error appears. After that, the identified NLOS distance is corrected by iteration correction in NICA shown in Fig.8. The modified distance matrix $\tilde{D}$ is accepted by NICA to approximate its original matrix until a threshold requirement is met. In our experiments, the threshold is set to 0.1. From the results in Table 4, we can see that the distance between node 1 and node 20 in Fig.7 is corrected from 120 to 56.54, the relative error of the corrected distance is 0.0096 (0.54/56). (21), as shown at the bottom of the previous page.

To verify the effect and validity of our proposed method, more experiments are carried out in the random topology network and the experimental results are provided in Table 4. In the algorithm, we use an interval $[d_l, d_h]$ to approximate the range of NLOS measurement d_{mn}. Each time we choose the center point of the interval to make two sub-intervals $[d_l, (d_l + d_h)/2]$ and $[d_l + d_h)/2, d_h]$, then we judge which sub-interval the true value of NLOS measurement is in from the signs of z_m and z_n. All the steps in the algorithm guarantee that the true value of NLOS measurement is in the sub-intervals which are getting smaller and smaller. Finally, when the range of the sub-interval is less than the threshold we set, the algorithm terminates and the true value of NLOS measurement is approximated by this interval.

Fig.12 presents the relationship between the corrected iteration number and the distance error size. In the case of low precision, our proposed algorithm quickly converges and the corrected result is close to the true value after 6 iterations.

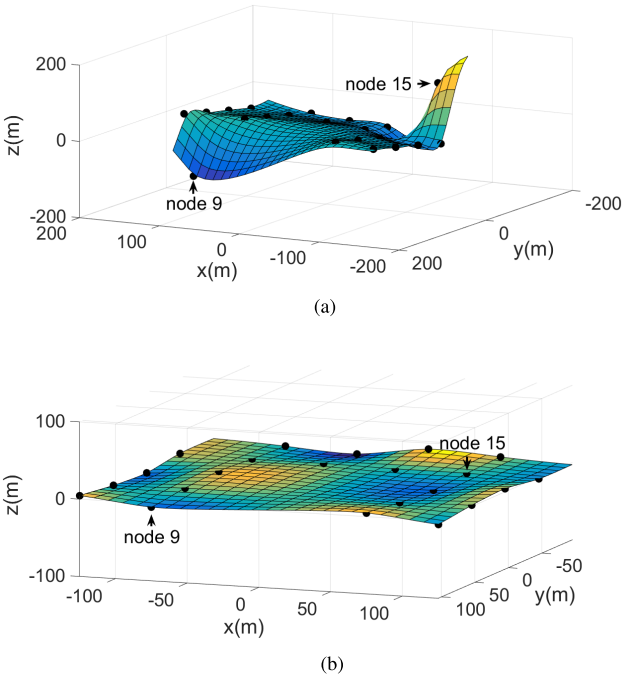

FIGURE 11. Comparison of C-type topological before and after correction. (a) before correction. (b) after correction.

The increase of the iteration number can not further improve the correction accuracy. We believe that the algorithm reaches the modified saturation at this time, and this saturation is actually determined by the constraints of the distance matrix $\tilde{D}$.

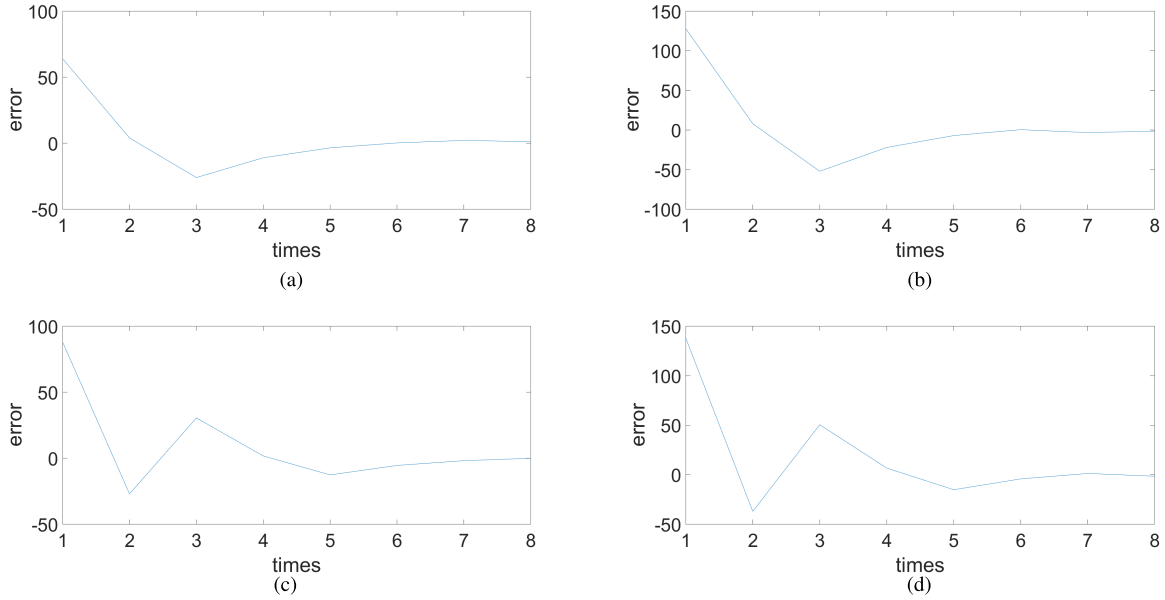

FIGURE 12. Correction efficiency. (a) random-type. (b) L-type. (c) grid-type. (d) C-type.

TABLE 4. Identification and correction of different position gross errors.

(Point1,Point2)	true value	value after gross error is introduced	identified results	corrected results
(1,20)	56	120	1,20	56.5430
(3,8)	101	160	3,8	98.8877
(11,13)	78	140	11,13	72.3219
(2,12)	100	150	2,12	97.6828
(5,9)	102	170	5,9	97.8662
(9,11)	60	100	9,11	57.9102
(5,6)	43	80	5,6	40.3906
(3,12)	55	100	3,12	57.4072
(14,17)	70	180	14,17	70.1560
(2,4)	88	200	2,4	88.4877
(6,15)	48	200	6,15	36.8673
(1,9)	85	240	1,9	84.2341

Therefore, in an actual system, we should balance the correction precision and the correction time.

V. CONCLUSION AND FUTURE WORK

In this paper, we explore the problem of NLOS identification and correction only using the constraints of distance matrix. We find that, if there is an NLOS measurement in 2-dimensional topologies, when we use MDS to derive coordinates from squared distance matrix in 3-dimensional space, we can identify the NLOS measurements in Z-domain using gross error detection methods such as QUAD. The proposed NLOS identification algorithm NIMQ is based on this important finding, and our experiments show the validity of NIMQ to identify NLOS measurements in different topologies. We find that performing MDS in a higher-dimensional space can harvest another property that could be used to correct the measured error. When the Z-coordinates of the NLOS measurement have opposite signs, it indicates that the measurement is longer than its true value and when they have the same sign, the measurement is shorter. The proposed NICA does NLOS correction based on this property. The experiments show that NICA can correct NLOS measurements very close to their true value, and the iteration converges quickly. The conclusion is based on the assumption that only one pair of NLOS distance is in the system, which will be extended in future work for identification and correction of multiple ones.

APPENDIX B PROOF OF LEMMA 1

From Equation 8-10, we have

$$-1/2P\tilde{D}^{(2)}P = \tilde{X}\tilde{X}'$$

Applying $\tilde{D^{(2)}} = D^{(2)} + \Delta D^{(2)}$ and $\tilde{X} = X + \Delta X$ to this equation yields

$$\|-1/2P(D^{(2)} + \Delta D^{(2)})P\|_2 = \|X + \Delta X\|_2^2$$

Thus,

$$\begin{aligned}|\|X+\Delta X\|_2^2-\|X\|_2^2| &= 1/2|\|P(D^{(2)}\\ &\quad +\Delta D^{(2)})P\|_2-\|PD^{(2)}P\|_2|\\ &\le 1/2\|P(D^{(2)}+\Delta D^{(2)})P-PD^{(2)}P\|_2\\ &= 1/2\|P\Delta D^{(2)}P\|_2\\ &\le 1/2\|P\|-2\|\Delta D^{(2)}\|-2\|P\|_2\\ &= 1/2|\|P\|_2^2\|\Delta D^{(2)}\|_2|\end{aligned}$$

It is easy to know that the eigenvalues of the real symmetric matrix P are $1,\ldots,1,0$, the eigenvalues of $P'P$ are $1^2,\ldots,1^2,0^2$, and $\|P\|_2=1$, therefore, (13) holds.

APPENDIX B
PROOF OF LEMMA 2

We define $e_t=(0,\cdots 1\cdots,0)$, where only the elements at t column are 1s, the rest of the elements are all 0s. Assuming $\tilde{X}_t$ is the t line of $\tilde{X}$, P_t is the t line of P, ΔX_t is the t line of ΔX. From Equation 8-10, we have

$$-1/2P\tilde{D}^{(2)}P=\tilde{X}\tilde{X}'$$

Multiplying both left and right sides by e_t gives

$$-1/2e_tP\tilde{D}^{(2)}Pe_t'=e_t\tilde{X}\tilde{X}'e_t'$$

or

$$-1/2P_t\tilde{D}^{(2)}P_t'=\tilde{X}_t\tilde{X}_t'$$

Therefore,

$$\|-1/2P_t\tilde{D}^{(2)}P_t'\|_2=\|\tilde{X}_t\tilde{X}_t'\|_2=\|\tilde{X}_t\|_2^2$$

Applying $\tilde{D^{(2)}}=D^{(2)}+\Delta D^{(2)}$ to this equation yields

$$\|-1/2P_t(D^{(2)}+\Delta D^{(2)})P_t'\|_2=\|(X_t+\Delta X_t)\|_2^2$$

Therefore,

$$\begin{aligned}|\|X_t+\Delta X_t\|_2^2-\|X_t\|_2^2| &= 1/2|\|P_t(D^{(2)}\\ &\quad +\Delta D^{(2)})P_t'\|_2-\|P_tD^{(2)}P_t'\|_2|\\ &\le 1/2\|P_t(D^{(2)}+\Delta D^{(2)})P_t'\\ &\quad -P_tD^{(2)}P_t'\|_2=1/2\|P_t\Delta D^{(2)}P_t'\|_2\end{aligned}$$

Since

$$\Delta D^2=\begin{pmatrix}0 & 0 & \cdots & 0\\ 0 & \ddots & \Delta d_{ij}^2 & 0\\ \vdots & \Delta d_{ij}^2 & \ddots & \vdots\\ 0 & 0 & \cdots & 0\end{pmatrix}$$

and

$$P_t=(-\frac{1}{n},\ldots,1-\frac{1}{n},\ldots,-\frac{1}{n})$$

we finally have (15).

REFERENCES

[1] G. Günther and C. Hoene, "Measuring round trip times to determine the distance between WLAN nodes," in *Proc. Int. Conf. Res. Netw.*, 2005, pp. 768–779.
[2] I. Borg and P. J. F. Groene, *Modern Multidimensional Scaling-Theory and Applications*, 2nd ed. New York, NY, USA: Springer, 2005.
[3] K. Bregar and M. Mohorčič, "Improving indoor localization using convolutional neural networks on computationally restricted devices," *IEEE Access*, vol. 6, pp. 17429–17441, 2018.
[4] J. K. Bullis, "Aberration correction by measurement and suppression of distortion waves," U.S. Patent 6 524 248 B1, Feb. 25, 2003.
[5] J. Caffery, "A new approach to the geometry of TOA location," in *Proc. 52nd Veh. Technol. Conf.*, Sep. 2000, pp. 1943–1949.
[6] B. E. B. Carvalho and N. G. Bretas, "Gross error processing in state estimation: Comparing the residual and the error tests," in *Proc. IEEE Manchester PowerTech*, Jun. 2017, pp. 1–5.
[7] L. Cheng, H. Wu, C. Wu, and Y. Zhang, "Indoor mobile localization in wireless sensor network under unknown NLOS errors," *Int. J. Distrib. Sensor Netw.*, vol. 9, no. 2, pp. 59–64, 2013.
[8] J.-S. Choi, W.-H. Lee, J.-H. Lee, J.-H. Lee, and S.-C. Kim, "Deep learning based NLOS identification with commodity WLAN devices," *IEEE Trans. Veh. Technol.*, vol. 67, no. 4, pp. 3295–3303, Apr. 2018.
[9] E. Elnahrawy, X. Li, and R. P. Martin, "The limits of localization using signal strength: A comparative study," in *Proc. 1st Annu. IEEE Commun. Soc. Conf. Sensor Ad Hoc Commun. Netw.*, Oct. 2004, pp. 406–414.
[10] I. Guvenc and C.-C. Chong, "A survey on TOA based wireless localization and NLOS mitigation techniques," *IEEE Commun. Surveys Tuts.*, vol. 11, no. 3, pp. 107–124, 3rd. Quart., 2009.
[11] Y. Liu, *Introduction to Internet Things*, 2nd ed. Beijing, China: Science Press, 2013.
[12] Y. Ma, B. Wang, S. Pei, Y. Zhang, S. Zhang, and J. Yu, "An indoor localization method based on AOA and PDOA using virtual stations in multipath and NLOS environments for passive UHF RFID," *IEEE Access*, vol. 6, pp. 31772–31782, 2018.
[13] B. Malila, O. Falowo, and N. Ventura, "Intelligent NLOS backhaul for 5G small cells," *IEEE Commun. Lett.*, vol. 22, no. 1, pp. 189–192, Jan. 2018.
[14] H. A. Mangalvedekar and S. D. Varwandkar, "Gross error identification in power system-a new method," in *Proc. 4th IEEE Region Int. Conf.*, Nov. 1989, pp. 782–785.
[15] A. A. Momtaz, F. Behnia, R. Amiri, and F. Marvasti, "NLOS identification in range-based source localization: Statistical approach," *IEEE Sensors J.*, vol. 18, no. 9, pp. 3745–3751, May 2018.
[16] W. J. Mullet and Y. Rodriguez, "System and related methods for detecting an obstruction in the path of a garage door controlled by an open-loop operator," U.S. Patent 5 929 580 A, Jul. 27, 1999.
[17] J. Ou, "Quasi Accurate Detection of gross errors (QUAD)," *ACTA Geodaetica ET Cartographic Sinica*, vol. 28, no. 1, pp. 15–20, 1999.
[18] A. T. Parameswaran, M. I. Husain, and S. Upadhyaya, "Is RSSI a reliable parameter in sensor localization algorithms: An experimental study," in *Proc. Field Failure Data Anal. Workshop (F2DA)*, New York, NY, USA, 2009.
[19] M. Ramadan, V. Sark, J. Gutierrez, and E. Grass, "NLOS identification for indoor localization using random forest algorithm," in *Proc. 22nd Int. ITG Workshop Smart Antennas*, Mar. 2018, pp. 1–5.
[20] A. Shrivastava and P. Bharti, "Localization techniques in wireless sensor networks," *Int. J. Comput. Appl.*, vol. 116, no. 12, pp. 13–18, 2015.
[21] Y. Shang and W. Ruml, "Improved MDS-based localization," in *Proc. IEEE INFOCOM*, vol. 4, Mar. 2004, pp. 2640–2651.
[22] Y. Shang, W. Ruml, Y. Zhang, and P. J. M. Fromherz, "Localization from mere connectivity," in *Proc. 4th ACM Int. Symp. Mobile Ad hoc Netw. Comput.*, 2003, pp. 201–212.
[23] D. Stojanović and N. Stojanović, "Indoor localization and tracking: Methods, technologies and research challenges. Facta universitatis," *Facta Universitatis, Ser., Autom. Control Robot.*, vol. 13, no. 1, pp. 57–72, 2014.
[24] J. Wang, Y. Ma, Y. Zhao, and K. Liu, "A multipath mitigation localization algorithm based on MDS for passive UHF RFID," *IEEE Commun. Lett.*, vol. 19, no. 9, pp. 1652–1655, Sep. 2015.
[25] X. Wang, Z. Wang, and B. O'Dea, "A TOA-based location algorithm reducing the errors due to non-line-of-sight (NLOS) propagation," *IEEE Trans. Veh. Technol.*, vol. 52, no. 1, pp. 112–116, Jan. 2003.
[26] C.-D. Wann, Y.-M. Chen, and M.-S. Lee, "Mobile location tracking with NLOS error mitigation," in *Proc. Global Telecommun. Conf.*, vol. 2, Nov. 2002, pp. 1688–1692.

[27] M. P. Wylie and J. Holtzman, "The non-line of sight problem in mobile location estimation," in *Proc. 5th Int. Conf. Universal Pers. Commun.*, vol. 2, Oct. 1996, pp. 827–831.
[28] L. Yan, Y. Lu, and Y. Zhang, "An improved NLOS identification and mitigation approach for target tracking in wireless sensor networks," *IEEE Access*, vol. 5, pp. 2798–2807, 2017.
[29] X. Yang, "NLOS mitigation for UWB localization based on sparse pseudo-input Gaussian process," *IEEE Sensors J.*, vol. 18, no. 10, pp. 4311–4316, May 2018.

YUHONG ZHU received the B.S. degree in wireless communication from the Changchun Post and Telecommunications College, Changchun, China, in 1993, the M.S. degree in communication and information systems from the Beijing University of Posts and Telecommunications, Beijing, China, in 2000, and the Ph.D. degree in communication and information systems from Jilin University, Changchun, in 2012.

From 2000 to 2005, he was a University Lecturer with the Department of Communications Engineering, Jilin University, where he is currently an Assistant Professor with the Department of Communications Engineering. His current research interests include wireless communication theory and applications, multimedia communications, and implementation and optimization of the algorithms in embedded systems.

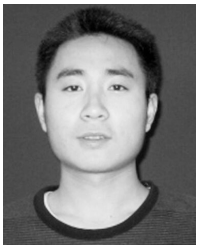

TENGFEI MA was born in Yantai, Shandong, China, in 1995. He received the B.S. degree in communication engineering from Jilin University, Changchun, China, in 2018, where he is currently pursuing the master's degree in information sensing and instrumentation with Zhejiang University, Hangzhou, China.

ZHIJUN LI received the B.S. degree in telecommunication engineering from the Changchun Post and Telecommunications College, Changchun, China, in 1997, and the M.S. degree in electronics and communication engineering from Jilin University, Changchun, China, in 2007, where he is currently a Senior Engineer with the Experimental Center. His current research interest includes mobile and pervasive computing, wireless communication and networks, and mobile applications.

DAYANG SUN was born in Nongan, Jilin, China, in 1979. He received the Ph.D. degree in computer science from Jilin University, China, in 2010.

From 2010 to 2018, he was a Lecturer with the College of Communication Engineering, Jilin University, where he is currently an Assistant Professor. His research interests includes lifetime assessing and energy aware technologies for wireless sensor networks, localization theory, and technologies for wireless networks.

XIAOSONG SUN received the M.S. and Ph.D. degrees in fundamental mathematics from the Department of Mathematics, Jilin University, Changchun, China, in 2002 and 2009, respectively.

From 2006 to 2013, he was a Lecturer with the Department of Mathematics, Jilin University, where he has been an Associate Professor since 2013. His research interests include affine algebraic geometry, and matrix theory and its applications.

Dr. Sun has been a Reviewer of *Mathematical Reviews* of American Mathematical Society, since 2012.

XIAOHUI ZHAO received the Ph.D. degree in control theory from the Universite de Technologie de Compiegne, France, in 1993. He is currently a Full Professor with the College of Communication Engineering, Jilin University, China. His current research interests include signal processing, wireless communication, and cognitive radio.

FENGYE HU received the B.S. degree from the Department of Precision Instrument, Xi'an University of Technology, China, in 1996, and the M.S. and Ph.D. degrees in communication and information systems from Jilin University, China, in 2000 and 2007, respectively.

He served as a Visiting Scholar in electrical and electronic engineering from Nanyang Technological University, Singapore, in 2011. He is currently a Full Professor with the College of Communication Engineering, Jilin University. His current research interests include wireless body area networks, wireless energy and information transfer, energy harvesting, cognitive radio, and space–time communication.

He has published 50 publications in IEEE journals and conferences. He organized the first and second Asia-Pacific Workshop on Wireless Networking and Communications (APWNC 2013 and APWNC 2015). He also organized the Future 5G Forum on Wireless Communications and Networking Big Data (FWCN 2016). He is currently serving as an Executive Co-Chairs of IEEE/CIC International Conference on Communications in China, China, in 2019. He is an Editor of *IET Communications* and *China Communications*, and is an Editor of *Physical Communication* on Special Issue on Ultra-Reliable, Low-Latency and Low-Power Transmissions in the Era of the Internet-of-Things.